



Echinacoside Protects Against MPP⁺-Induced Neuronal Apoptosis via ROS/ATF3/CHOP Pathway Regulation

Qing Zhao¹ · Xiaoyan Yang² · Dingfang Cai^{3,4} · Ling Ye^{5,6} · Yuqing Hou¹ · Lijun Zhang¹ · Jiwei Cheng¹ · Yuan Shen¹ · Kaizhe Wang⁵ · Yu Bai¹

Received: 25 October 2015 / Accepted: 24 May 2016 / Published online: 18 July 2016

© Shanghai Institutes for Biological Sciences, CAS and Springer Science+Business Media Singapore 2016

Abstract Echinacoside (ECH) is protective in a mouse model of Parkinson's disease (PD) induced by 1-methyl-4-phenylpyridinium ion (MPP⁺). To investigate the mechanisms involved, SH-SY5Y neuroblastoma cells were treated with MPP⁺ or a combination of MPP⁺ and ECH, and the expression of ATF3 (activating transcription factor 3), CHOP (C/EBP-homologous protein), SCNA (synuclein alpha), and GDNF (glial cell line-derived neurotrophic factor) was assessed. The results showed that ECH significantly improved cell survival by inhibiting the

generation of MPP⁺-induced reactive oxygen species (ROS). In addition, ECH suppressed the ROS and MPP⁺-induced expression of apoptotic genes (*ATF3*, *CHOP*, and *SCNA*). ECH markedly decreased the MPP⁺-induced caspase-3 activity in a dose-dependent manner. ATF3-knockdown also decreased the CHOP and cleaved caspase-3 levels and inhibited the apoptosis induced by MPP⁺. Interestingly, ECH partially restored the GDNF expression that was down-regulated by MPP⁺. ECH also improved dopaminergic neuron survival during MPP⁺ treatment and protected these neurons against the apoptosis induced by MPTP. Taken together, these data suggest that the ROS/ATF3/CHOP pathway plays a critical role in mechanisms by which ECH protects against MPP⁺-induced apoptosis in PD.

Electronic supplementary material The online version of this article (doi:10.1007/s12264-016-0047-4) contains supplementary material, which is available to authorized users.

✉ Qing Zhao
qingzhao2010@hotmail.com

✉ Yu Bai
baiyu_bb@sina.com

¹ Department of Neurology, Putuo Hospital, Shanghai University of Traditional Chinese Medicine, Shanghai 200062, China

² Department of Emergency Internal Medicine, Putuo Hospital, Shanghai University of Traditional Chinese Medicine, Shanghai 200062, China

³ Laboratory of Neurology, Institute of Integrative Medicine, Zhongshan Hospital, Fudan University, Shanghai 200032, China

⁴ Department of Integrative Medicine, Zhongshan Hospital, Fudan University, Shanghai 200032, China

⁵ Center for Translational Neurodegeneration and Regenerative Therapy, Shanghai Tenth People's Hospital Affiliated with Tongji University School of Medicine, Shanghai 200072, China

⁶ Department of Immunology, Tongji University School of Medicine, Shanghai 200092, China

Keywords Echinacoside · Parkinson's disease · 1-Methyl-4-phenylpyridinium ion · Reactive oxygen species · ATF3 · CHOP

Introduction

Parkinson's disease (PD) is the second most common neurodegenerative disorder, characterized by slowly progressive and selective loss of dopamine (DA) neurons in the substantia nigra pars compacta (SNc) and a reduction in striatal DA levels [1]. Pathological studies have shown that the development of PD is associated with genetic and environmental factors. The first gene to be associated with inherited PD is that for α -synuclein (*SNCA*). However, mutations of leucine-rich repeat kinase 2 (*LRRK2*) and parkin are the most common causes of inherited PD [2]. It is well known that alternate forms of α -synuclein are involved in the pathology of PD, and reactive oxygen

species (ROS) also contribute to its development [3]. Characteristics similar to PD can be induced by several environmental toxins, including 1-methyl-4-phenyl-1,2,3,6-tetrahydropyridine (MPTP), cyanide, carbon disulfide, and toluene. MPTP is widely used to induce animal models of PD, and its active metabolite, 1-methyl-4-phenylpyridinium ion (MPP⁺), is used in cell models of PD [4, 5]. MPP⁺ selectively inhibits the electron transport chain and results in excessive ROS production, thereby inducing neuronal death and a syndrome resembling PD [6]. Recent studies have shown that MPP⁺ induces multiple pathways in an *in vitro* PD model, including increased GSK3B phosphorylation (pY206) and α -synuclein accumulation [5], upregulation of the heme oxygenase-1/nicotinamide adenine dinucleotide phosphate oxidase/ROS axis [7, 8], increased expression of active transcription factor 3 (ATF3), and growth arrest *via* DNA damage-inducible 153 (GADD153)/C/EBP-homologous protein (CHOP) [9]. In clinical treatment, suppression of ROS products is one of the most important strategies for the survival of neurons and the treatment of PD [1].

Echinacoside (ECH, Fig. 1A), a natural phenylethanoid found in many medicinal plants, is a principal constituent of the phenylethanoid glycosides isolated from the traditional Chinese herb, *Cistanche salsa* [10]. Interestingly, recent studies have shown that ECH has protective effects in a mouse model of PD induced by MPTP [10, 11]. ECH also attenuates neuroblastoma cell apoptosis induced by tumor necrosis factor- α or 6-hydroxydopamine *in vitro* [12, 13]. However, the mechanisms by which ECH promotes the survival of neurons in the MPP⁺-induced PD cell model remain unclear.

We showed that ECH markedly reduced the ROS products induced by MPP⁺ in SH-SY5Y cells. ECH also inhibited the MPP⁺-induced expression of ATF3, CHOP, and α -synuclein, as well as suppressing activation of the pro-apoptosis proteins caspase-3 and poly (ADP-ribose) polymerase (PARP).

Materials and Methods

Reagents

Dulbecco's minimal essential medium (DMEM), fetal bovine serum, 0.25% trypsin, 1% penicillin/streptomycin, and TRIzol reagent were from Life Technologies (Grand Island, NY). The chromatin dye bisbenzimidazole (Hoechst 33342), poly-L-lysine, MPP⁺ iodide, and MPTP were from Sigma (St. Louis, MO). The lipid peroxidation malondialdehyde (MDA) assay kit and dichlorofluorescein diacetate (DCFH-DA) were from Beyotime Biotech (Haimen, China). ECH of $\geq 98\%$ purity was from Push Bio-technology (Chengdu, China).

Animals and Treatments

Animal maintenance and treatments were as described previously [14]. We used male C57BL/6 mice (Shanghai Laboratory Animal Co., Shanghai, China) weighing 24–26 g at 10 weeks of age. The animals were maintained under standard conditions (12:12 h light:dark cycle, 21 \pm 2°C, and relative humidity 40%) and allowed access to food and water *ad libitum*. All procedures were approved by the Animal Ethics Committee of Zhongshan Hospital, Fudan University and carried out in accordance with the National Institutes of Health Guide for the Care and Use of Laboratory Animals.

Mice were randomly divided into four groups (10 mice/group): group A, vehicle control group, given an equal volume (500 μ L) of normal saline (NS); group B, ECH control group, given 20 mg/kg ECH; group C, MPTP model group, pre-treated with an equal volume of NS; and group D, ECH-treated group, pre-treated with 20 mg/kg ECH. ECH was dissolved in NS and delivered by intragastric administration every 24 h for 15 consecutive days. The mouse PD model for groups C and D was generated by five consecutive intraperitoneal injections of 30 mg/kg MPTP every 24 h from day 11 to day 15. Mice were killed by cervical dislocation or perfusion being narcotized by 10% chloralhydrate (3.6 mg/kg) intraperitoneally 24 h after the final treatment.

Perfusion and tissue processing were as described previously [14]. After intracardiac perfusion, brain samples were collected and fixed in 4% paraformaldehyde for 24 h at 4°C, embedded in paraffin, and coronal sections encompassing the entire SNc (stereotaxic coordinates antero-posterior -3.64 to -2.92 mm relative to bregma) were cut at 5 μ m.

Another 5 animals from each group were killed by cervical dislocation and the ventral midbrain was rapidly lysed in 1% SDS lysis buffer on ice. CHOP and ATF3 protein levels in the lysate were analyzed by western blotting.

Culture of Rat Ventral Midbrain (VM)

Dopaminergic Neurons

Pregnant Wistar rats were purchased from the Shanghai Laboratory Animal Co., (Shanghai, China). DA neurons in the VM were isolated on embryonic day 14. The VM was dissected and processed for establishing primary VM DA neuron cultures as previously described [15, 16]. In brief, tissue pieces were collected in ice-cold Hanks' balanced salt solution (HBSS) and centrifuged at 1000 rpm at 4°C for 5 min. The tissue pellet was incubated in 750 μ L of 0.1% trypsin-HBSS for 15 min at 37°C with 5% CO₂. Fetal calf serum (FCS; 750 μ L) was used to inactivate trypsin and tissues were dissociated by gentle trituration

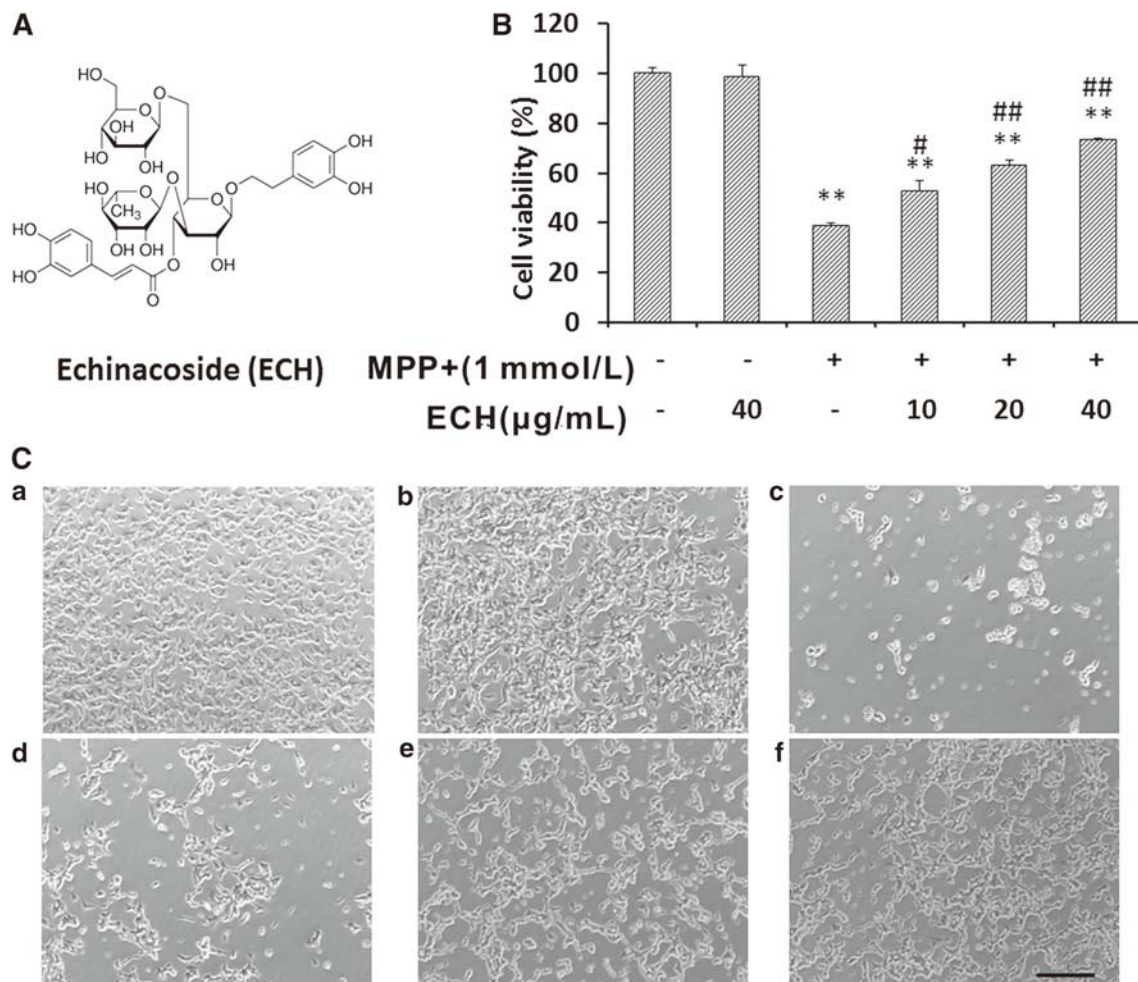


Fig. 1 Echinacoside inhibits MPP⁺-induced apoptosis in SH-SY5Y cells. **A** Chemical structure of echinacoside (Pusi Biotechnology Company). **B** Effects of echinacoside on viability with or without MPP⁺. SH-SY5Y cells were plated into 96-well plates, incubated overnight, and then fed fresh medium each day with the indicated drugs; viability was analyzed after 3 days. Data from three independent experiments were normalized to the results from control cells

and are presented as mean \pm SD ($n = 6$; ** $P < 0.01$ vs control, # $P < 0.05$, ## $P < 0.01$ vs MPP⁺ treatment). **C** Light microscopic images of morphological changes induced by MPP⁺ or MPP⁺ and ECH. a, PBS control; b, 40 μ g/mL ECH; c, 1 mmol/L MPP⁺; d, 1 mmol/L MPP⁺ and 10 μ g/mL ECH; e, 1 mmol/L MPP⁺ and 20 μ g/mL ECH; f, 1 mmol/L MPP⁺ and 40 μ g/mL ECH (scale bar, 200 μ m).

using a sterilized Pasteur pipette. Cell suspensions were centrifuged at 1000 rpm for 4 min at 4°C and re-suspended in differentiation medium (Dulbecco's modified Eagle's medium/F12, 33 mmol/L D-glucose, 1% L-glutamine, and 1% FCS, supplemented with 2% B27). Cells were seeded on poly-D-lysine (Sigma)-coated 24-well tissue culture plates at 5×10^4 cells/well in 500 μ L differentiation medium at 37°C with 5% CO₂ for 10 days to develop into mature DA neurons. VM DA neurons were characterized by immunofluorescence with anti- β -tubulin isotype III antibody and tyrosine hydroxylase (TH) antibody (Fig. S1). Cells were treated with 1 mmol/L MPP⁺, 40 μ g/mL ECH, a combination of MPP⁺ and ECH, or PBS alone as control. Cell viability was analyzed with CCK-8 reagent after 96 h of treatment.

SH-SY5Y Cell Culture

SH-SY5Y cells were from the Cell Bank of Shanghai Institute of Cell Biology (Chinese Academy of Sciences, Shanghai, China) and cultured in DMEM supplemented with 10% fetal bovine serum, 100 U/mL penicillin, and 100 U/mL streptomycin. Cells were maintained in a humidified 37°C incubator supplied with 5% CO₂. MPP⁺ was dissolved in sterile water and used immediately. ECH was dissolved in PBS. To explore ROS-related gene expression and protein levels, cells were seeded into 6-well plates and cultured for 24 h. The cells were then fed with fresh medium containing MPP⁺, ECH, a combination of MPP⁺ and ECH, or PBS alone as control. After 24 h of treatment, the cells were lysed with 1% SDS lysis buffer (1% SDS,

25 mmol/L EDTA, 45 mmol/L Tris-HCl, pH 6.5) for western blot analysis, and total RNA was isolated directly with TRIzol reagent.

To analyze the ATF3 and CHOP distribution after treatment, nuclear and cytoplasmic extraction reagent kits (Thermo Fisher, Waltham, MA) were used to extract cytoplasmic and nuclear fractions from drug-treated and control cells.

Cell Viability Assay

SH-SY5Y cells were seeded into 96-well plates and incubated overnight. The cells were fed every 24 h with fresh complete medium containing different drugs and maintained for 3 days. Then viability was assessed using the CCK8 cell counter kit (Dojindo, Japan). Data were normalized to results from the PBS control and are presented as mean \pm SD. To analyze viability in ATF3-knockdown SH-SY5Y (ATF3 shRNA) and control (GFP shRNA) cells, the cells were added to 96-well plates and cultured for 14–16 h. ATF3 shRNA or GFP shRNA plasmids were transfected into SH-SY5Y cells using Lipofectamine 2000 (Life Technologies, Carlsbad, CA). The cells were treated with 1 mmol/L MPP⁺ or an equal volume of PBS after 24 h of transfection and were then incubated for 3 days. Cell numbers were counted every day. Data are presented as mean \pm SD.

shRNA Constructs and Oligo Primers

pGV298-ATF3 shRNA (ATF3shRNA) and GFP control shRNA constructs were from GeneChem Co. (Shanghai, China). The ATF3 target sequence was 5'-GCAAAGT G!CCGAAACAAGA-3' from previously-described methods [17, 18]. To detect gene expression induced by MPP⁺, ROS stress-related and PD-associated genes were selected for qRT-PCR, and GAPDH was used as the control. All primers were synthesized by Sangon Biotech Co. (Shanghai, China), and the primer sequences are listed in Table 1.

Real-Time PCR

Total RNA was extracted with TRIzol reagent according to the manufacturer's instructions. Reverse-transcription and quantitative real-time PCR (qRT-PCR) were performed as previously described. The reverse transcription reaction was performed using the RevertAid First Strand cDNA Synthesis kit (Thermo Scientific, Waltham, MA) according to the manufacturer's instructions. The SYB Premix Ex Taq II kit (TaKaRa, Dalian, China) was used for qRT-PCR: 20- μ L reaction systems were used with ABI (Life Technologies, Carlsbad, CA). The PCR parameters comprised the following steps: 95°C for 3 min, 1 cycle; 95°C for 5 s and 60°C for 40 s, 40 cycles. The final data were normalized to GAPDH and are presented as a ratio to control. The primers used for amplification are listed in Table 1.

Western Blotting

Western blot analysis was performed as previously described [19]. The primary antibodies were anti-cleaved caspase 3 and p53 (Cell Signaling Technology, Danvers, MA), anti-GAPDH (Proteintech Group, Chicago, IL), anti-GADD153/CHOP (Wanlei Bio, Shenyang, China), and anti-ATF3, anti-PARP, anti-PUMA and anti-histone 3 (Santa Cruz Biotechnology, Santa Cruz, CA). Horseradish peroxidase-labeled secondary antibodies were from Jackson Immune Research Laboratories (Western Grove, PA). The PVDF membranes were from EMD Millipore (Billerica, MA) and the ECL substrate was from CWBio (Suzhou, China). Relative protein levels based on gray levels from the image were analyzed with Tanon GIS software (Tanon Biotech, Shanghai, China), and data are presented as the ratio of target protein to GAPDH.

Immunofluorescence Staining

SH-SY5Y cells grown on polylysine-coated coverslips were fixed with cold methanol after 24 h of treatment with

Table 1 Primers for qRT-PCR

Gene accession No.	Gene ID	Primer	Sequence
NM_001030287	ATF3	Forward	CGAAGACTGGAGCAAATG ATG
		Reverse	CATCCAGGCCAGGTCTCTGCCTCAG
NM_001195053	DDIT3 (CHOP)	Forward	TGCTTTCAGGTGTGGTGATG TATG
		Reverse	AATCAGAGCTGGAACCTGAGGA
NM_000514	GDNF	Forward	TGACAAAGTAGGGCAGGCATGT
		Reverse	ATCCACACCTTTTAGCGGAATGC
NM_000345	SCNA	Forward	CCCTCCGAGAGCGTCCT
		Reverse	ACACCACACTGTGTCGAAT
NM_001256799	GAPDH	Forward	CTCAGACACCATGGGGAAG GTGA
		Reverse	ATGATCTTGAGGCTGTTGCATA

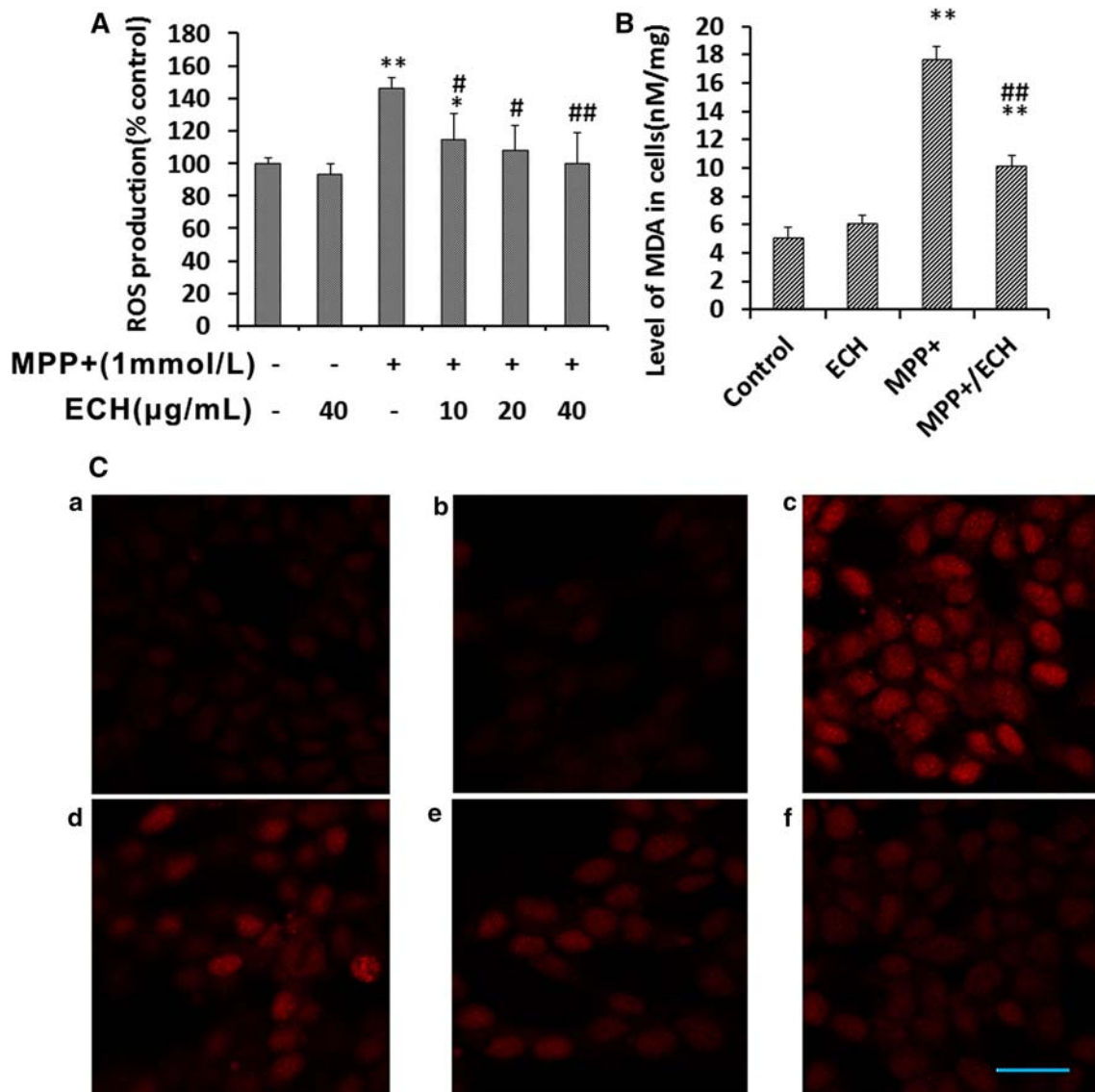


Fig. 2 Echinacoside decreases MPP⁺-induced ROS production in SH-SY5Y cells. **A** Effects of ECH on MPP⁺-induced ROS products. Cells were seeded into 96-well plates, cultured overnight, and then treated as indicated for 24 h. DCFH-DA (10 μmol/L) was used to analyze ROS levels. Data were normalized to the control group and are presented as mean ± SD ($n = 6$; * $P < 0.05$, ** $P < 0.01$; # $P < 0.05$, ## $P < 0.01$ vs MPP⁺ treatment). **B** ECH blocked the MPP⁺-induced increase of MDA expression. Cells were incubated with indicated drugs for 24 h. Control, PBS; ECH, 40 μg/mL; MPP⁺,

1 mmol/L; MPP⁺/ECH, 1 mmol/L MPP⁺ and 40 μg/mL ECH. Data were normalized to the control group and are presented as mean ± SD ($n = 6$; ** $P < 0.01$ vs control; # $P < 0.05$, ## $P < 0.01$ vs MPP⁺ treatment). **C** Representative fluorescence microscopic images of ROS expression in cells treated with different drugs for 24 h, then incubated with 10 μmol/L DCFH-DA for 20 min. a, PBS control; b, 40 μg/mL ECH; c, 1 mmol/L MPP⁺; d, 1 mmol/L MPP⁺ and 10 μg/mL ECH; e, 1 mmol/L MPP⁺ and 20 μg/mL ECH; f, 1 mmol/L MPP⁺ and 40 μg/mL ECH (scale bar, 25 μm).

1 mmol/L MPP⁺, 40 μg/mL ECH, or a combination of MPP⁺ and ECH. The cells were then incubated in blocking buffer (3% BSA in PBS) at room temperature (RT) for 30 min. Then, anti-ATF3, anti-CHOP, or anti-cleaved caspase 3 antibodies were diluted to 1:100 in blocking buffer (1% BSA in PBS with 0.3% Triton X-100) and incubated overnight at 4°C. After washing three times with PBS, the cells were incubated with Alexa[®]488-goat anti-rabbit IgG (Life Technologies, Carlsbad, CA) at RT for

1 h. Nuclei were stained with Hoechst 33342. Images were captured with a confocal microscope (Leica SP8, Wetzlar, Germany).

Terminal Deoxynucleotidyl Transferase-Mediated dUTP Nick-End Labeling (TUNEL) Assay

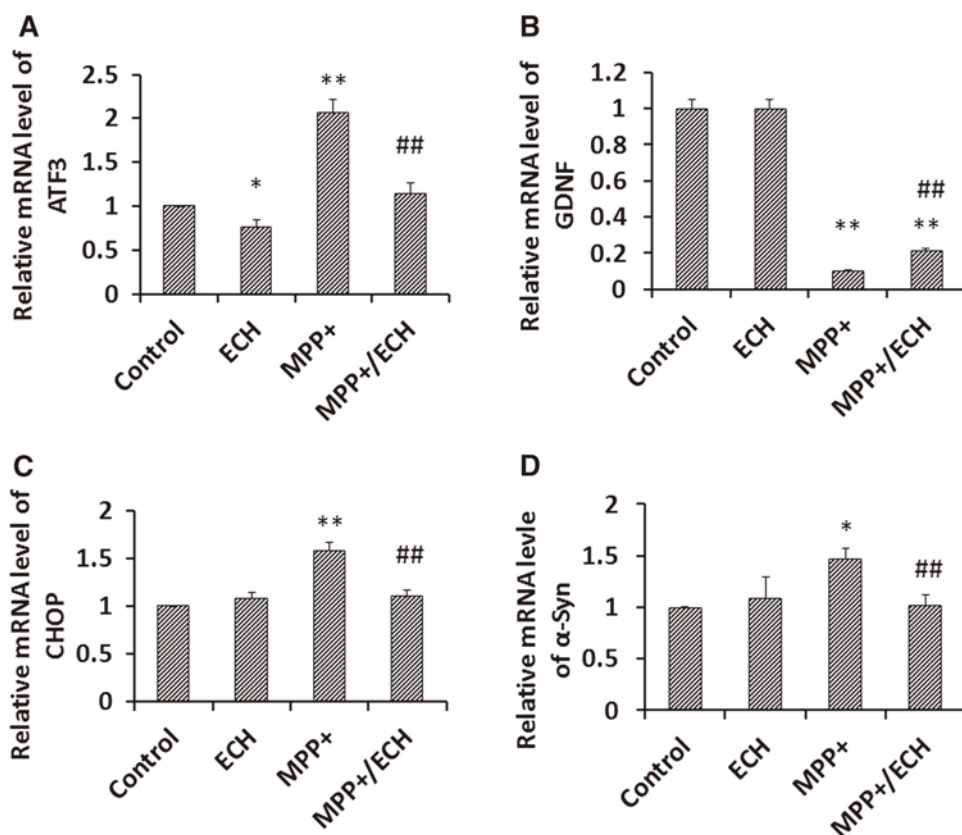
We stained every 10th coronal section (total 14–15) through the SNc from bregma −2.92 mm to −3.64 mm.

Four typical sections through the SNc at the same level in each group were used for TH and TUNEL counts [10]. TUNEL assays were performed to analyze apoptosis in tissue sections with an in situ cell death detection kit (Roche, Rotkreuz, Switzerland), following the manufacturer's instructions. After DNA labeling, sections were used for immunofluorescence staining with anti-TH antibody, and images were captured with a confocal microscope (Leica SP8, Wetzlar, Germany). After delineation of the SNc at low magnification (10 × objective) according to the mouse brain atlas [20], the TH-positive cells and TH/TUNEL double-positive cells were counted at a higher magnification (20 × objective) by two observers blind to the treatment. The ratio of TH/TUNEL double-positive cells to TH-positive cells was calculated.

Statistical Analysis

All data are presented as mean ± SD. One-way ANOVA followed by post hoc analysis with Tukey's HSD and the Student–Newman–Keuls multiple comparisons test were performed for statistical purposes. A value of $P < 0.05$ was considered statistically significant.

Fig. 3 Echinacoside regulates expression of ROS stress- and survival-related genes induced by MPP⁺ in SH-SY5Y cells. qRT-PCR analysis of target mRNA expression (A ATF3; B GDNF; C CHOP; D α -Syn). Cells plated in 6-well plates and cultured for 24 h were then treated as indicated for 24 h. Data from three independent experiments were normalized to the PBS control group. Data are presented as mean ± SD ($n = 3$; Control, PBS; ECH, 40 μ g/mL; MPP⁺, 1 mmol/L; MPP⁺/ECH, 1 mmol/L MPP⁺ and 40 μ g/mL ECH; * $P < 0.05$, ** $P < 0.01$ vs control; # $P < 0.05$, ## $P < 0.01$ vs ECH).



Results

ECH Decreases ROS Products and Attenuates MPP⁺-Induced Apoptosis

ECH has been shown to protect neurons from apoptosis in animal models, as well as reducing the levels of pro-inflammatory cytokines in neuroblastoma cells [12]. However, it remains unclear whether ECH directly modulates the neuronal apoptosis induced by MPP⁺. Our data showed that ECH did not affect the proliferation or death of SH-SY5Y cells (Fig. 1B), and their morphology remained unchanged (Fig. 1C). Interestingly, following exposure of SH-SY5Y cells to MPP⁺, survival increased in a dose-dependent manner after ECH treatment (10–40 μ g/mL) (Fig. 1B,C).

Previous studies have shown that MPP⁺ specifically inhibits electron transport chain in mitochondria and is also associated with ROS generation [6, 21]. Using DCFH-DA as a fluorescent probe to assess changes in ROS levels, we found that ECH markedly suppressed the MPP⁺-induced ROS generation (Fig. 2A). Confocal microscopy revealed that the decreased ROS products were associated with ECH levels (Fig. 2C). ECH was also shown to protect the cell membrane against ROS and decrease MDA levels, the end product of lipid peroxidation (Fig. 2B). Taken together,

ECH promotes cell survival by decreasing MPP⁺-induced ROS products in neurons.

ECH Suppresses ROS Stress-Related/MPP⁺-Induced Gene Expression and Increases GDNF Expression in MPP⁺-Treated Cells

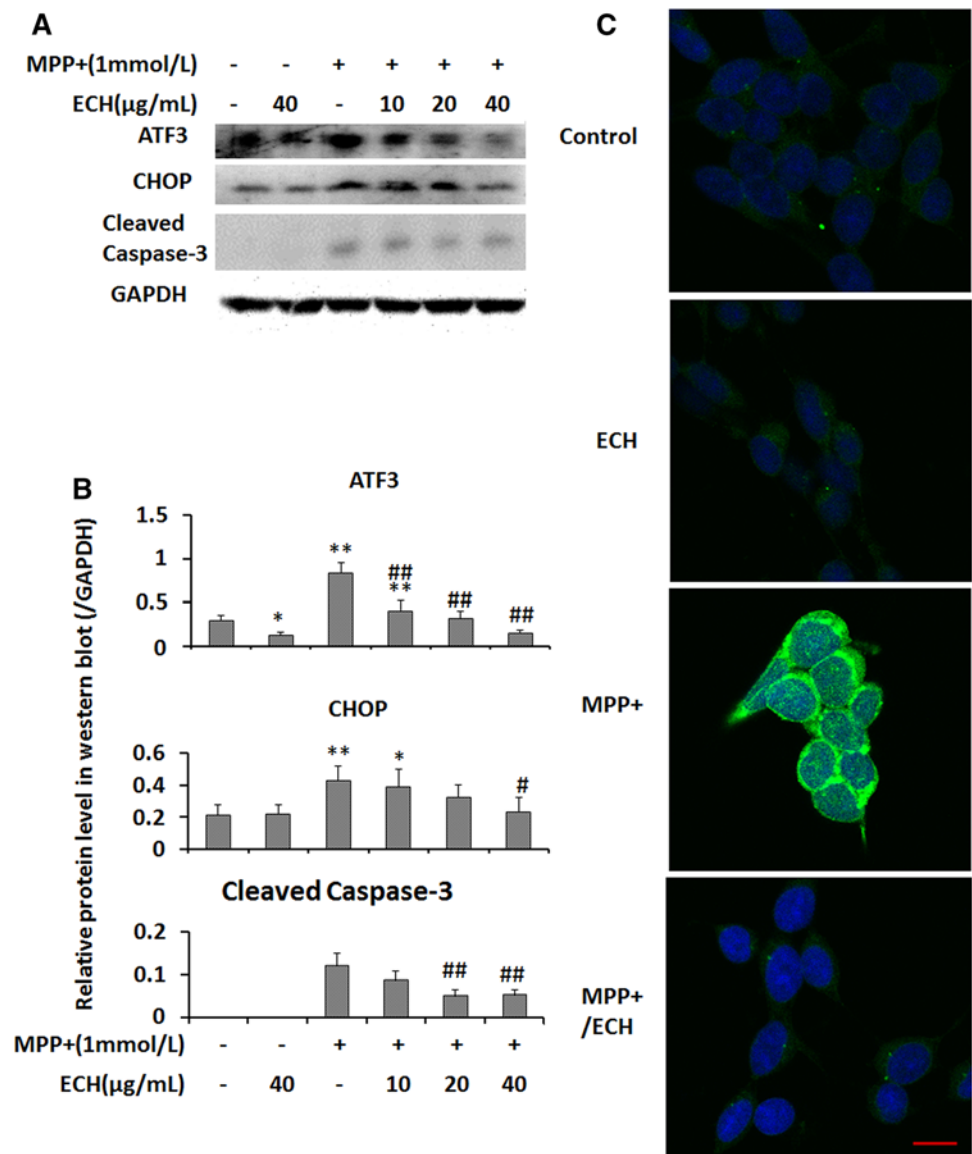
ROS products have been shown to stimulate the unfolded protein response and induce the expression of stress-related genes, including *ATF3*, *ATF4*, and *CHOP* [22]. *ATF3* and *CHOP* play an especially important role in stress-induced neuronal apoptosis [9, 23]. Abnormal α -synuclein expression is also one of the critical markers in PD pathology [2]. Using qRT-PCR, we analyzed the expression of *ATF3*, *CHOP*, *SNCA*, and glial cell line-derived neurotrophic factor (*GDNF*) in the MPP⁺ cell model and found that

MPP⁺ significantly enhanced the expression of *ATF3*, *CHOP*, and *SNCA* compared with the PBS control group. ECH did not affect expression of these genes in SH-SY5Y cells that were not treated with MPP⁺. However, ECH abrogated their MPP⁺-induced expression (Fig. 3). In addition, MPP⁺ significantly suppressed the expression of *GDNF* in SH-SY5Y cells, but ECH partially reversed this phenomenon (Fig. 3B).

ECH Inhibits MPP⁺-Induced Caspase-3 Activation in SH-SY5Y Cells

High levels of *ATF3* and *CHOP* directly promote neuronal apoptosis [9, 23]. Our data showed that ECH inhibited *ATF3* and *CHOP* expression in a dose-dependent manner (Fig. 4A). ECH also blocked MPP⁺-induced caspase-3

Fig. 4 Echinacoside downregulates ROS stress-related and pro-apoptotic proteins in SH-SY5Y cells. **A** Western blots of *ATF3*, *CHOP*, and cleaved caspase-3 protein from cells treated as indicated for 24 h. **B** Statistics of relative protein levels as in (A). Data are presented as mean \pm SD of the ratio of the indicated protein to GAPDH ($n = 3$). **C** Immunofluorescence images showing that ECH suppressed the caspase-3 activation induced by MPP⁺ (Control, PBS; ECH, 40 μ g/mL; MPP⁺, 1 mmol/L; MPP⁺/ECH, 1 mmol/L MPP⁺ and 40 μ g/mL ECH; scale bar, 10 μ m).



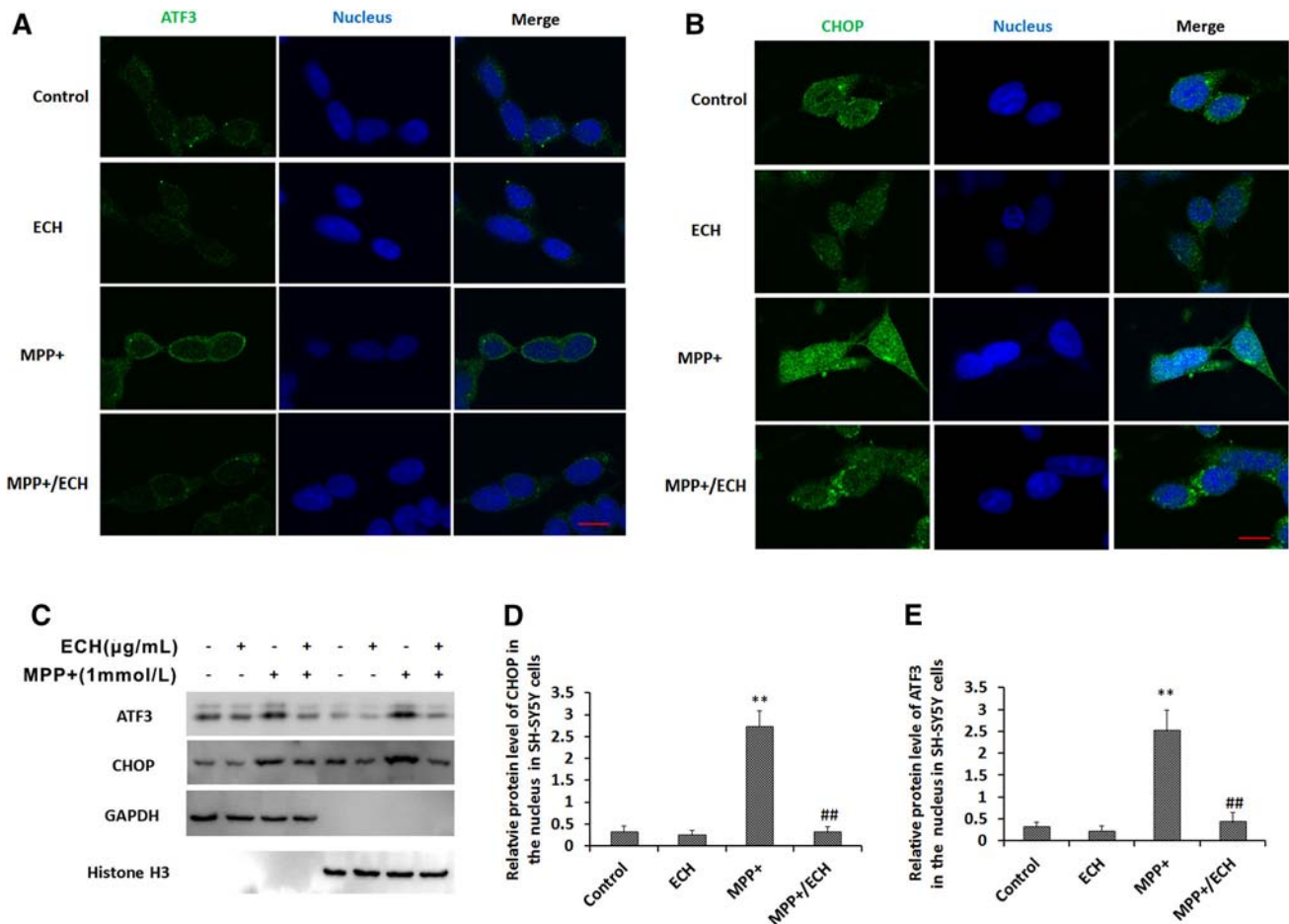


Fig. 5 Echinacoside decreases nuclear expression of ATF3 and CHOP proteins induced by MPP⁺ in SH-SY5Y cells. **A, B** Images of cells stained for endogenous ATF3 (green in A) and CHOP (green in B). Alexa[®]488-goat anti-rabbit IgG and Hoechst 33342 were sequentially used to stain each target protein and nuclei (blue). Scale

bar, 10 μ m. **C** Western blots of ATF3 and CHOP proteins in the cytoplasmic and nuclear fractions. **D, E** Statistics for experiments as in (C). Data are presented as mean \pm SD of the ratio of the indicated protein to histone3 ($n = 3$; ** $P < 0.01$ vs control group, ## $P < 0.01$ vs MPP⁺ group).

activity (Fig. 4A, B). Immunofluorescence analysis of the cleaved form of caspase-3 further showed that ECH markedly decreased the cleaved caspase-3 protein expression in MPP⁺-treated cells (Fig. 4C).

ECH Reverses MPP⁺-Induced ATF3 and CHOP Accumulation in SH-SY5Y Cells

Following exposure to environmental toxins, ATF3 and CHOP proteins localize in the cytoplasm and nucleus [24, 25], and this leads to apoptosis. Our results suggested that MPP⁺ treatment increased ATF3 and CHOP expression in the nucleus, and ECH effectively attenuated this process (Fig. 5A, B). Western blotting analysis showed that MPP⁺ markedly increased levels of both proteins in the cytoplasm and nucleus. Interestingly, ECH abrogated the MPP⁺ effects and suppressed ATF3 and CHOP accumulation in the nucleus (Fig. 5C–E).

ATF3 Plays a Critical Role in MPP⁺-Induced Apoptosis in SH-SY5Y Cells

ATF3 has been shown to induce apoptosis in SH-SY5Y cells [23], and the results from the present study indicate that ECH significantly suppresses ATF3 mRNA and protein expression induced by MPP⁺ in these cells. However, the role of ATF3 in apoptosis and ECH protection of cell survival remained unclear. So we used small hairpin RNA (shRNA) specific for ATF3 to investigate this and found no difference in viability between the ATF3-knockdown group and the control group under normal conditions (Fig. 6A). However, ATF3 suppression or ECH treatment significantly rescued the morphological changes induced by MPP⁺ (Fig. 6B). The ATF3-knockdown cells had higher viability than the control group following exposure to MPP⁺ (Fig. 6C). The protein levels of CHOP and activated caspase-3 were lower in ATF3-knockdown cells than

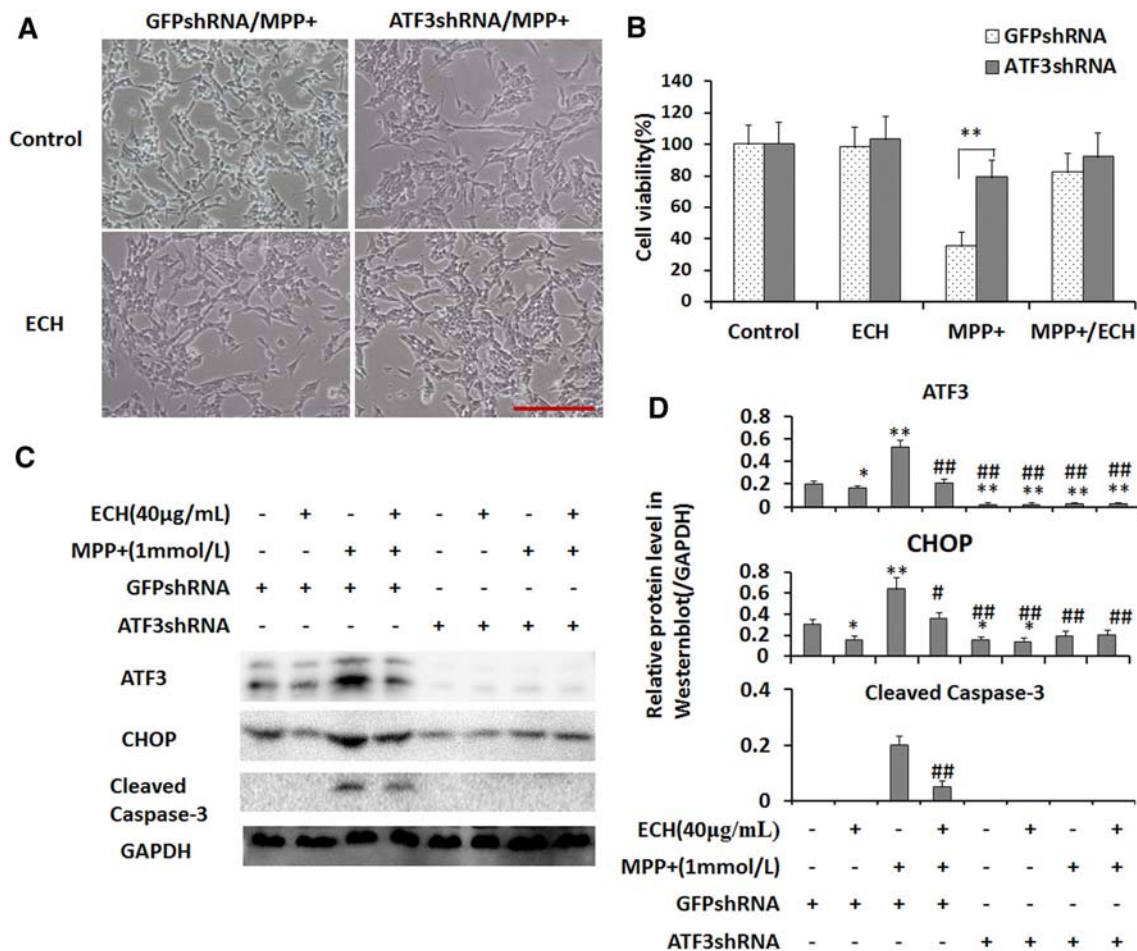


Fig. 6 ATF3 plays a critical role in the action of ECH against MPP⁺-induced apoptosis *via* the ROS stress pathway in SH-SY5Y cells. **A** Downregulation of ATF3 attenuates morphological changes induced by MPP⁺. Light microscopic images of ATF3 knock-down and control cells after 24-h treatment as indicated (Control, PBS and 1 mmol/L MPP⁺; ECH, 40 µg/mL ECH and 1 mmol/L MPP⁺, scale

bar, 200 µm). **B** Cell viability normalized to the control group. Data are presented as mean ± SD (*n* = 6; ***P* < 0.01). **C** Western blots of ATF3, CHOP, and cleaved caspase-3 proteins with GAPDH serving as the loading control. **D** Statistics for experiments as in (C). Data are presented as mean ± SD of the ratio of the indicated protein to GAPDH (*n* = 3).

in control cells with non-specific shRNA (Fig. 6C, D). These data indicated that ATF3 plays a critical role in the MPP⁺-induced apoptosis of neuroblastoma cells. So, these results support the hypothesis that ECH protects SH-SY5Y cells against MPP⁺-induced effects *via* downregulation of the ROS/ATF3/CHOP pathway. Interestingly, our data showed that ECH also inhibited the MPP⁺-induced increase of p53 and PUMA (p53-upregulated modulator of apoptosis) levels in SH-SY5Y cells (Fig. 7).

ECH Protects DA Neurons Against Apoptosis Induced by MPP⁺ *in Vitro* or by MPTP *in Vivo*

To confirm the action of ECH in PD, primary DA neurons were treated with MPP⁺ or MPP⁺ and ECH. The *in vitro* experiments revealed that MPP⁺ significantly reduced the viability of DA neurons and this was prevented by ECH

(Fig. 8). We further assessed apoptosis in DA neurons in the SNc after different treatments in mice with MPTP-induced PD and controls. More TH-positive neurons were found in this area in the control than in the MPTP group (Fig. 9A). TUNEL assays showed that NS and ECH did not induce apoptosis in DA neurons in the SNc, but MPTP did and ECH protected the neurons against it (Figs. 9B, S2). Interestingly, western blotting of lysates of the SNc from the mouse model of PD showed that the ATF3 and CHOP protein levels were also decreased by ECH (Fig. 10).

Discussion

ECH is one of the most active phenylethanoid glycosides involved in anti-oxidant and free-radical scavenging [26]. Several studies have shown that it significantly improves

Fig. 7 Echinacoside downregulates p53 and PUMA in SH-SY5Y cells. **A** Western blots of p53 and PUMA proteins in cells treated as indicated for 24 h. GAPDH served as loading control. **B, C** Statistics for experiments as in (A). Data are presented as mean \pm SD of the ratio of the indicated protein to GAPDH ($n = 3$; Control, PBS; ECH, 40 $\mu\text{g}/\text{mL}$; MPP⁺, 1 mmol/L; MPP⁺/ECH, 1 mmol/L MPP⁺ and 40 $\mu\text{g}/\text{mL}$ ECH).

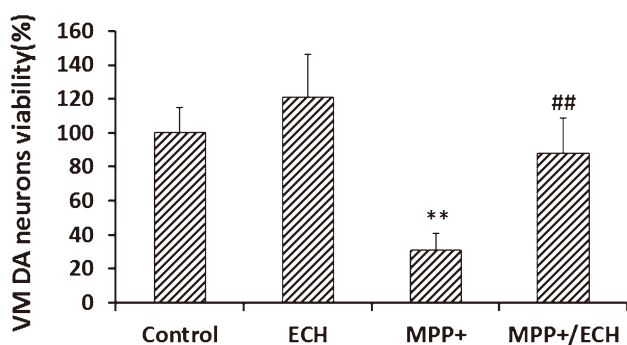
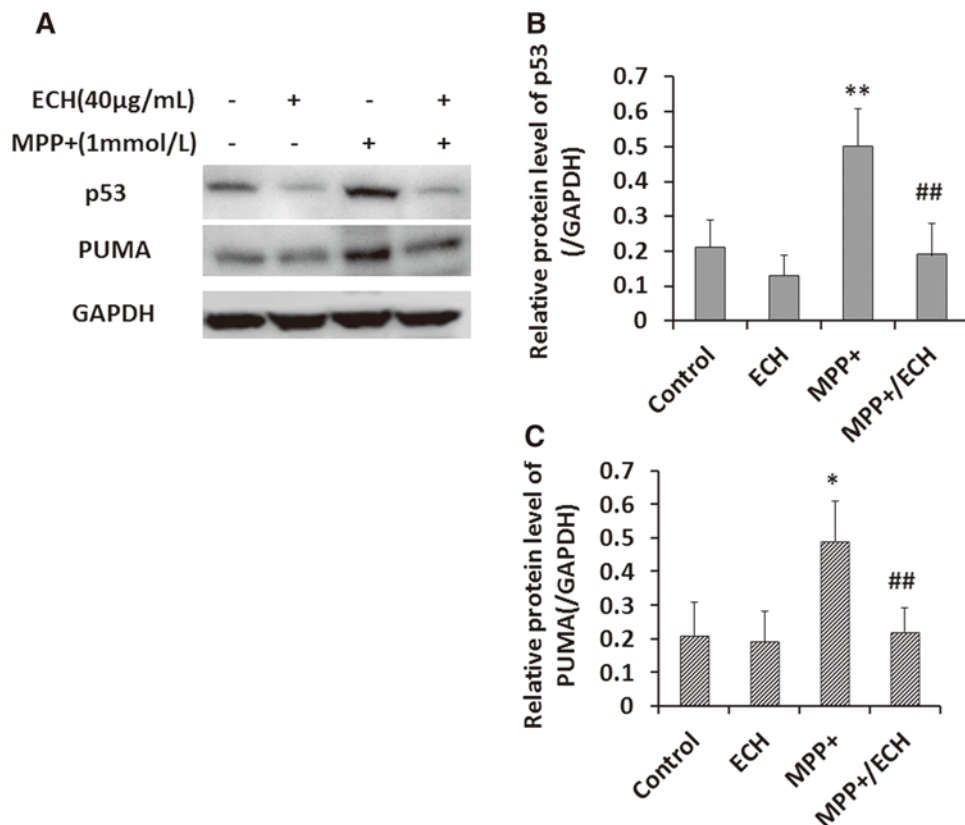


Fig. 8 ECH protects primary DA neurons *in vitro*. Viability of rat primary VM DA neurons treated as indicated. Data from three independent experiments normalized to the results from control cells and presented as mean \pm SD ($n = 6$; ** $P < 0.01$).

motor behavior and suppresses the loss of nigral DA neurons in MPTP-lesioned mice. Other results have shown that ECH protects neurons by inhibiting active caspase-3/8 in cerebellar granule cells and enhancing the expression of GDNF and brain-derived neurotrophic factor in the SNc [10, 11]. Data from the present study demonstrated that ECH directly inhibits MPP⁺-induced ROS production in SH-SY5Y neuroblastoma cells. ROS is one of products of cellular energy metabolism. Under normal conditions, superoxide dismutase and other anti-oxidants guard against

and inhibit the accumulation of ROS [27]. It is well known that mitochondria are the main source of cellular ROS, and ROS generation is associated with mitochondrial morphology and function [28]. Recent studies have reported that mitochondrial damage and ROS products may be involved in MPP⁺-induced apoptosis in SH-SY5Y cells [7, 29]. Current studies have suggested that protecting mitochondrial structure or mitochondrial processes abrogates the apoptosis induced by MPP⁺ [29, 30]. Several studies have demonstrated that ECH protects cell survival in different PD models *via* blocking the mitochondrial damage induced by MPP⁺ [13, 21]. A recent study showed that MPP⁺ is partly responsible for the necrosis in SH-SY5Y cells [31]. In primary DA neurons, MPP⁺ induces necrosis by increasing the expression and secretion of TNF- α and IL-1 β and reducing the expression and secretion of insulin-like growth factor-1 [32]. Many studies suggest that apoptosis is the dominant cause of MPP⁺-induced SH-SY5Y cell death. Our data also strongly supported this hypothesis (Figs. 4, 9).

Cells that are consistently exposed to excessive ROS can develop serious issues, including damage to the lipid membrane system, changes in protein translation and folding, and increased genome instability [33]. Finally, excessive ROS induces the transcription of apoptosis-associated genes, ultimately resulting in apoptosis or death

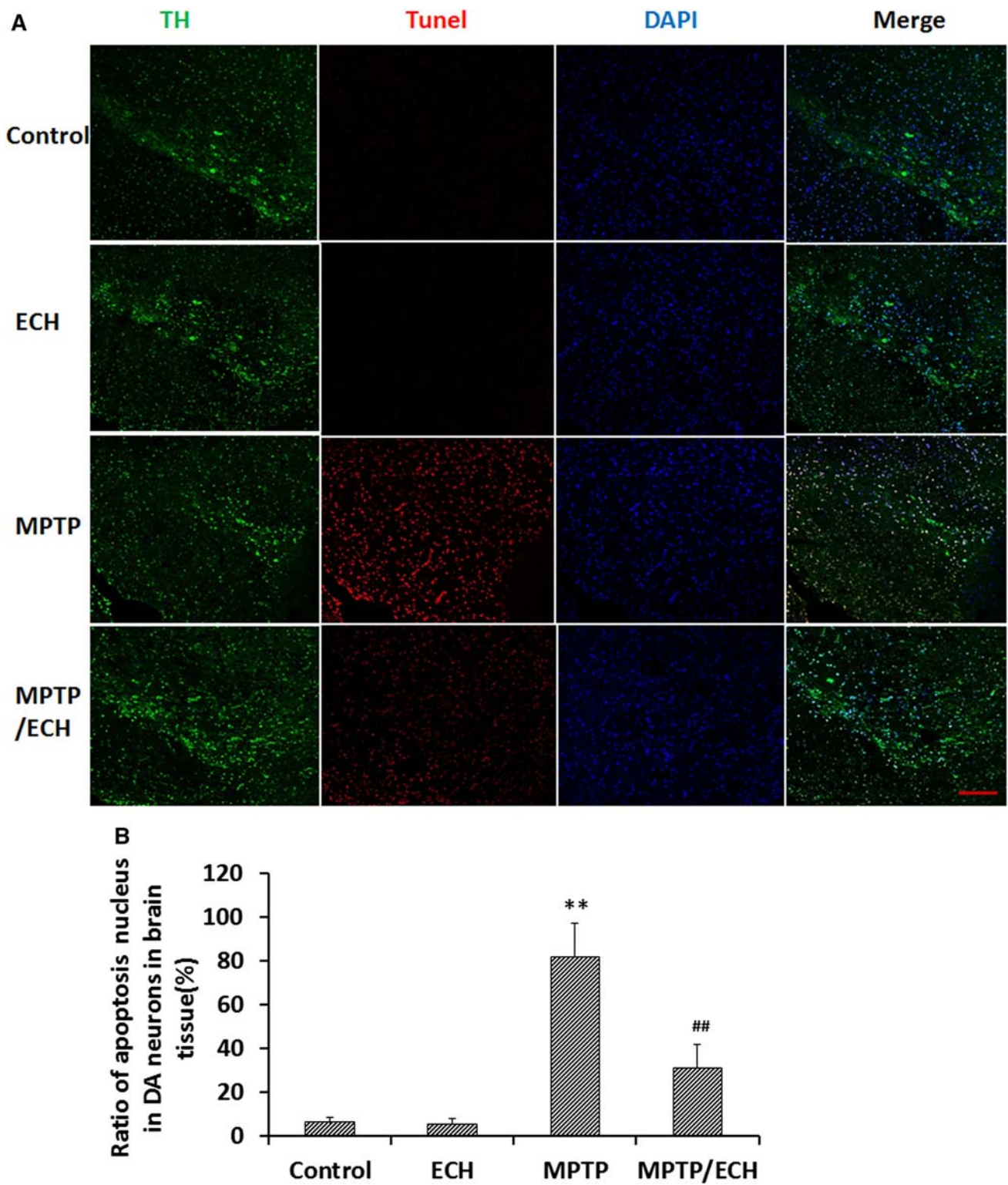
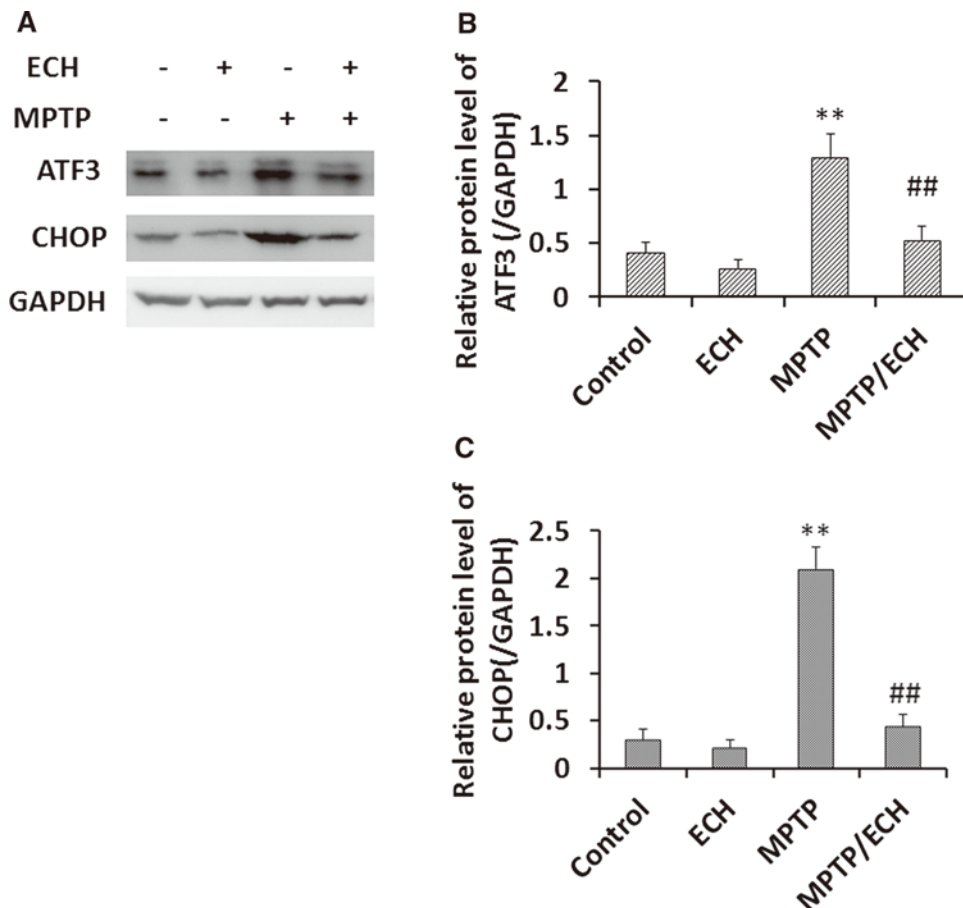


Fig. 9 ECH blocks DA neuronal apoptosis in mouse PD model. **A** Immunofluorescence and TUNEL assay images of apoptotic TH-positive (TH⁺) cells in sections through the substantia nigra pars compacta. Nuclei were stained with DAPI (blue). TH⁺ cells (green)

and TH⁺ and TUNEL-positive nuclei (red) were counted (scale bar, 200 μm). **B** Ratios of apoptotic DA neurons. Data are presented as mean ± SD (*n* = 5; ***P* < 0.01 vs control group; ##*P* < 0.01 vs MPP⁺ group).

Fig. 10 ECH suppresses ATF3 and CHOP expression in mouse PD model. **A** Western blots of ATF3 and CHOP proteins in lysates of mouse SNc tissue, with GAPDH serving as the loading control. **B, C** Statistics for experiments as in (A). Data are presented as mean ± SD of the ratio of the indicated protein to GAPDH ($n = 5$).



[34, 35]. *ATF3* and *CHOP* are two of the most critical genes for ROS-induced stress responses. Recent studies have shown MPP⁺-induced ATF3 and CHOP expression in neuroblastoma cells [9, 23]. ATF3 upregulates p53 expression and induces apoptosis in SH-SY5Y cells [23] and other cells [17, 36]. Interestingly, a recent study showed that ATF3 upregulation of p53 plays an important role in apoptosis induced by MPP⁺ [36]. CHOP was first identified as a transcription factor that is induced in response to growth arrest and DNA damage. ATF3 regulates CHOP expression and associates with CHOP to modulate apoptosis [37, 38]. Our results showed that ECH effectively suppressed ATF3 expression with or without MPP⁺ (Fig. 3A) and also inhibited MPP⁺-induced apoptosis (Fig. 4A). Besides CHOP, ECH also suppressed p53 and PUMA expression in the cellular model of PD (Fig. 7). These results suggest that ECH plays a role in the modulation of ATF3 expression.

Our results also showed that ATF3 down-regulation by shRNA significantly attenuated CHOP expression and the cleaved caspase-3 level that were previously induced by MPP⁺ (Fig. 6C). This suggests that ATF3 plays a role in the MPP⁺-induced apoptosis of SH-SY5Y cells. In

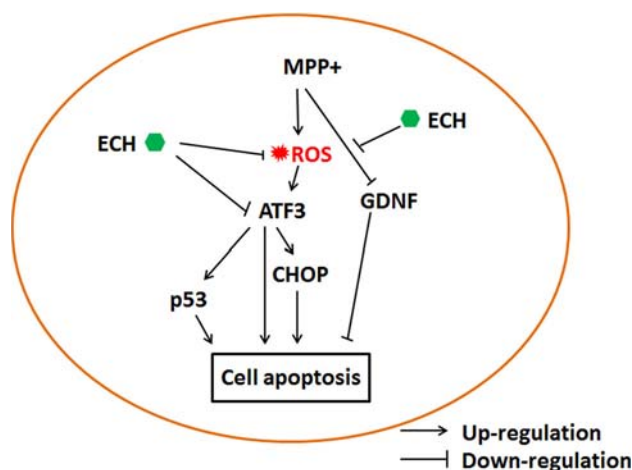


Fig. 11 Proposed mechanisms underlying the protective actions of ECH against MPP⁺-induced apoptosis in SH-SY5Y cells. ECH attenuates the ROS formation induced by MPP⁺, and in turn downregulates the expression of ATF3 and CHOP. ECH also directly inhibits ATF3 expression. Another branch shows that ECH promotes the expression of the anti-apoptosis protein, GDNF, in MPP⁺-treated cells. ATF3 regulates expression of the pro-apoptosis proteins p53 in the PD cell model as well. All of these actions contribute to the protective effect of ECH against apoptosis induced by MPP⁺.

addition, the results showed that ECH improved GDNF expression following MPP⁺ treatment in SH-SY5Y cells (Fig. 3B). GDNF is an important pro-survival factor for neurons [14]. These *in vitro* results are consistent with data from animal models [14].

Taken together, the results from the present study demonstrate that the ROS/ATF3/CHOP pathway plays a critical role in the protective mechanisms of ECH against DA cell apoptosis induced by MPP⁺, revealing a novel mechanism for ECH neuroprotection in an *in vitro* model of PD (Fig. 11).

Acknowledgments This work was supported by the National Natural Science Foundation of China (81202814), the Shanghai Municipal Commission of Health and Family Planning (20124y116) and the Young Teachers Training Funding Scheme of Shanghai Colleges and Universities, China (zszs12026). We thank Dr. Yunsheng Yuan, Professor Dazheng Wu, and Associate Professor Peihao Yin for their guidance on the experiments and preparation of the manuscript.

References

- Kalia LV, Lang AE. Parkinson's disease. *Lancet* 2015, 386: 896–902.
- Lees AJ, Hardy J, Revesz T. Parkinson's disease. *Lancet* 2009, 373: 2055–2066.
- Pagonabarraga J, Kulisevsky J, Strafella AP, Krack P. Apathy in Parkinson's disease: clinical features, neural substrates, diagnosis, and treatment. *Lancet Neurol* 2015, 14: 518–531.
- Lehri-Boufala S, Ouidja MO, Barbier-Chassefiere V, Henault E, Raïsmann-Vozari R, Garrigue-Antar L, *et al.* New roles of glycosaminoglycans in alpha-synuclein aggregation in a cellular model of Parkinson disease. *PLoS One* 2015, 10: e0116641.
- Duka T, Duka V, Joyce JN, Sidhu A. Alpha-Synuclein contributes to GSK-3beta-catalyzed Tau phosphorylation in Parkinson's disease models. *FASEB J* 2009, 23: 2820–2830.
- Zhang ZG, Wu L, Wang JL, Yang JD, Zhang J, Li LH, *et al.* Astragaloside IV prevents MPP(+)-induced SH-SY5Y cell death via the inhibition of Bax-mediated pathways and ROS production. *Mol Cell Biochem* 2012, 364: 209–216.
- Lee DH, Kim CS, Lee YJ. Astaxanthin protects against MPTP/MPP⁺-induced mitochondrial dysfunction and ROS production in vivo and in vitro. *Food Chem Toxicol* 2010, 49: 271–280.
- Ye Q, Huang B, Zhang X, Zhu Y, Chen X. Astaxanthin protects against MPP(+)-induced oxidative stress in PC12 cells via the HO-1/NOX2 axis. *BMC Neurosci* 2013, 13: 156.
- Conn KJ, Gao WW, Ullman MD, McKeon-O'Malley C, Eisenhauer PB, Fine RE, *et al.* Specific up-regulation of GADD153/CHOP in 1-methyl-4-phenyl-pyridinium-treated SH-SY5Y cells. *J Neurosci Res* 2002, 68: 755–760.
- Zhao Q, Gao J, Li W, Cai D. Neurotrophic and neurorescue effects of Echinacoside in the subacute MPTP mouse model of Parkinson's disease. *Brain Res* 2010, 1346: 224–236.
- Geng X, Tian X, Tu P, Pu X. Neuroprotective effects of echinacoside in the mouse MPTP model of Parkinson's disease. *Eur J Pharmacol* 2007, 564: 66–74.
- Deng M, Zhao JY, Tu PF, Jiang Y, Li ZB, Wang YH. Echinacoside rescues the SHSY5Y neuronal cells from TNFalpha-induced apoptosis. *Eur J Pharmacol* 2004, 505: 11–18.
- Wang YH, Xuan ZH, Tian S, Du GH. Echinacoside Protects against 6-Hydroxydopamine-Induced Mitochondrial Dysfunction and Inflammatory Responses in PC12 Cells via Reducing ROS Production. *Evid Based Complement Alternat Med* 2015, 2015: 189–239.
- Zhao Q, Cai D, Bai Y. Selegiline rescues gait deficits and the loss of dopaminergic neurons in a subacute MPTP mouse model of Parkinson's disease. *Int J Mol Med* 2013, 32: 883–891.
- Lingor P, Unsicker K, Kriegelstein K. Midbrain dopaminergic neurons are protected from radical induced damage by GDF-5 application. Short communication. *J Neural Transm (Vienna)* 1999, 106: 139–144.
- Hegarty SV, Collins LM, Gavin AM, Roche SL, Wyatt SL, Sullivan AM, *et al.* Canonical BMP-Smad signalling promotes neurite growth in rat midbrain dopaminergic neurons. *Neuro-molecular Med* 2014, 16: 473–489.
- Wang H, Mo P, Ren S, Yan C. Activating transcription factor 3 activates p53 by preventing E6-associated protein from binding to E6. *J Biol Chem* 2010, 285: 13201–13210.
- Weng S, Zhou L, Deng Q, Wang J, Yu Y, Zhu J, *et al.* Niclosamide induced cell apoptosis via upregulation of ATF3 and activation of PERK in Hepatocellular carcinoma cells. *BMC Gastroenterol* 2016, 16: 25.
- Yuan Y, Zhang X, Weng S, Guan W, Xiang D, Gao J, *et al.* Expression and purification of bioactive high-purity recombinant mouse SPP1 in Escherichia coli. *Appl Biochem Biotechnol* 2014, 173: 421–432.
- Franklin Keith BJ, Paxinos G. *The Mouse Brain in Stereotaxic Coordinates*. 3rd ed. San Diego: Academic Press, 2007: 52–63.
- Zhu M, Zhou M, Shi Y, Li WW. Effects of echinacoside on MPP(+)-induced mitochondrial fragmentation, mitophagy and cell apoptosis in SH-SY5Y cells. *Journal of Chinese Integrative Medicine* 2012, 10: 1427–1432.
- Wang WA, Groenendyk J, Michalak M. Endoplasmic reticulum stress associated responses in cancer. *Biochim Biophys Acta* 2014, 1843: 2143–2149.
- Tian Z, An N, Zhou B, Xiao P, Kohane IS, Wu E. Cytotoxic diarylheptanoid induces cell cycle arrest and apoptosis via increasing ATF3 and stabilizing p53 in SH-SY5Y cells. *Cancer Chemother Pharmacol* 2009, 63: 1131–1139.
- Hai T, Wolfgang CD, Marsee DK, Allen AE, Sivaprasad U. ATF3 and stress responses. *Gene Expr* 1999, 7: 321–335.
- Li Y, Guo Y, Tang J, Jiang J, Chen Z. New insights into the roles of CHOP-induced apoptosis in ER stress. *Acta Biochim Biophys Sin (Shanghai)* 2015, 47: 146–147.
- Heilmann J, Calis I, Kirmizibekmez H, Schuhly W, Harput S, Sticher O. Radical scavenger activity of phenylethanoid glycosides in FMLP stimulated human polymorphonuclear leukocytes: structure-activity relationships. *Planta Med* 2000, 66: 746–748.
- Indo HP, Yen HC, Nakanishi I, Matsumoto K, Tamura M, Nagano Y, *et al.* A mitochondrial superoxide theory for oxidative stress diseases and aging. *J Clin Biochem Nutr* 2015, 56: 1–7.
- Willems PH, Rossignol R, Dieteren CE, Murphy MP, Koopman WJ. Redox Homeostasis and Mitochondrial Dynamics. *Cell Metab* 2015, 22: 207–218.
- Yang L, Zhao K, Calingasan NY, Luo G, Szeto HH, Beal MF. Mitochondria targeted peptides protect against 1-methyl-4-phenyl-1,2,3,6-tetrahydropyridine neurotoxicity. *Antioxid Redox Signal* 2009, 11: 2095–2104.
- Cartelli D, Ronchi C, Maggioni MG, Rodighiero S, Giavini E, Cappelletti G. Microtubule dysfunction precedes transport impairment and mitochondria damage in MPP⁺-induced neurodegeneration. *J Neurochem* 2010, 115: 247–258.
- Jantas D, Greda A, Golda S, Korostynski M, Grygier B, Roman A, *et al.* Neuroprotective effects of metabotropic glutamate receptor group II and III activators against MPP(+)-induced cell death in human neuroblastoma SH-SY5Y cells: the impact of cell differentiation state. *Neuropharmacology* 2014, 83: 36–53.

32. Liu Z, Chen HQ, Huang Y, Qiu YH, Peng YP. Transforming growth factor-beta1 acts via TbetaR-I on microglia to protect against MPP(+)-induced dopaminergic neuronal loss. *Brain Behav Immun* 2016, 51: 131–143.
33. Smeyne M, Smeyne RJ. Glutathione metabolism and Parkinson's disease. *Free Radic Biol Med* 2013, 62: 13–25.
34. Wei R, Zhang R, Xie Y, Shen L, Chen F. Hydrogen Suppresses Hypoxia/Reoxygenation-Induced Cell Death in Hippocampal Neurons Through Reducing Oxidative Stress. *Cell Physiol Biochem* 2015, 36: 585–598.
35. Jiang H, Ren Y, Zhao J, Feng J. Parkin protects human dopaminergic neuroblastoma cells against dopamine-induced apoptosis. *Hum Mol Genet* 2004, 13: 1745–1754.
36. Khwanraj K, Phruksaniyom C, Madlah S, Dharmasaroja P. Differential Expression of Tyrosine Hydroxylase Protein and Apoptosis-Related Genes in Differentiated and Undifferentiated SH-SY5Y Neuroblastoma Cells Treated with MPP⁺. *Neurol Res Int* 2015, 2015: 734703. (Add doi or add pages!).
37. Jiang HY, Wek SA, McGrath BC, Lu D, Hai T, Harding HP, *et al.* Activating transcription factor 3 is integral to the eukaryotic initiation factor 2 kinase stress response. *Mol Cell Biol* 2004, 24: 1365–1377.
38. Xu L, Su L, Liu X. PKCdelta regulates death receptor 5 expression induced by PS-341 through ATF4-ATF3/CHOP axis in human lung cancer cells. *Mol Cancer Ther* 2012, 11: 2174–2182.